THERMAL OVERSTABILITY OF HYDROMAGNETIC SURFACE WAVES

P. S. JOARDER*, M. H. GOKHALE, and P. VENKATAKRISHNAN

*Indian Institute of Astrophysics, Bangalore 560034, India***

(Received 11 November, 1986; in revised form 8 May, 1987)

Abstract. We investigate the effects of radiative heat losses and thermal conductivity on the hydromagnetic surface waves along a magnetic discontinuity in a plasma of infinite electrical conductivity. We show that the effects of radiative heat losses on such surface waves are appreciable only when values of the plasma pressure on the two sides of the discontinuity are substantially different. Overstability of a surface wave requires that the medium in which it gives larger first-order compression should satisfy the criterion of Field (1965). Possible applications of the study to magnetic discontinuities in solar corona are briefly discussed.

1. Introduction

Hydromagnetic surface waves in magnetically structured plasma media have been studied extensively by Wentzel (1979a, b), Roberts (1981a, b), Edwin and Roberts (1982), Somasundaram and Uberoi (1982), and Somasundaram (1983). They have shown that a single surface of discontinuity separating two uniform, magnetic and compressible plasma media can sustain in general two hydromagnetic surface waves propagating along the interface and evanescent on both sides of the interface. Dissipation of such waves are believed to contribute to the irreversible heating of the solar coronal plasma (Ionson, 1978, 1985; Wentzel, 1979c; Rae and Roberts, 1981; Gordon and Hollweg, 1983). In view of the increasing awareness of their importance for the energetics of the upper solar atmosphere, an examination of the thermal stability of such surface waves in the presence of different heat gain and loss mechanisms is necessary.

A detailed discussion of the physics of the thermal instability can be found in Field (1965). For an optically thin, uniform medium, one gets an exponentially growing isobaric or isochoric instability mode as well as two overstably oscillating, nearly isentropic-acoustic modes propagating in opposite directions. Thermal conductivity stabilizes these modes for wavelengths smaller than some critical wavelength. In the presence of a uniform, frozen-in magnetic field, condensations with wavevector perpendicular to the field get stabilized for the field strength exceeding a certain critical value while the condensations along the field remain unaffected. Among the three MHD wave modes, the Alfvén mode, being incomrpessible, is thermally neutral while the overstability criterion for the compressible slow and the fast MHD modes remains same as that for the acoustic mode, although their growthrates get modified by the magnetic field.

* Collaborative programme in Astronomy and Astrophysics, Department of Physics, Indian Institute of Science, Bangalore 560012, India.
** Mailing address.

Solar Physics **110** (1987) 255–270.

Thermal instability in magnetohydrodynamic media has been further discussed by many authors in the context of their application to the solar atmospheric situations (see, for example, Heyvaerts, 1974; Hildner, 1974; Priest, 1978; An, 1984; Bodo *et al.*, 1986). These authors have considered either the role of condensation modes in the formation of magnetic structures or the stability of existing structures against condensation and bulk MHD perturbations. In the present paper, we investigate the effects of radiative losses and thermal conductivity on the fast and the slow hydromagnetic surface modes along a discontinuity separating two semi-infinite magnetic plasma media. We consider modes with wavevectors along the field direction. In Section 2 we state the basic equations and derive the relevant dispersion relation. In Section 3 we discuss the asymptotic behaviour of the dispersion relation. Numerical solution of the dispersion equation in two different cases using parameters typical of solar atmosphere are presented in Section 4. We find that each of the slow and the fast compressible surface waves will be overstable or decaying depending on the radiative properties of the two media to different extents. We also find that the thermal conductivity parallel to the magnetic field introduces a cut-off in the wavelength for the onset of overstability of the surface modes. In Section 5, we briefly summarize our results and discuss its relevance to the study of the solar coronal structures.

2. Derivation of the Dispersion Relation

2.1. Basic Equations

The basic set of equations consists of the usual MHD equations. The gas is assumed to be perfect and completely ionized (with mean molecular weight = $\frac{1}{2}$). In the energy equation we include a heating term in a phenomenological way, a radiative cooling term corresponding to an optically thin medium and a term representing the divergence of the thermal flux due to an anisotropic thermal conductivity. The rate of heating per unit volume is assumed to be proportional to the density and independent of the temperature of the medium. For radiative cooling rate per unit volume we use the formula given by Rosner *et al.* (1978). We further assume the magnetic field to be frozen into the plasma. In a low-density, high-temperature plasma with strong magnetic field, like the solar coronal plasma, we can ignore the thermal conductivity perpendicular to the magnetic field (Spitzer, 1962) and for the numerical value of the parallel conductivity, we use the formula given by Priest (1982). Thus, we take:

$$K_{\parallel} = 9 \times 10^{-7} T^{5/2} \text{ ergs s}^{-1} \text{ cm}^{-1} \text{ K}^{-1} . \tag{1}$$

The basic equations (in conventional notations) then reduce to the following.

The fluid dynamical equations, viz.,

$$\mathrm{d}\rho/\mathrm{d}t + \rho(\nabla \cdot \mathbf{v}) = 0 ; \tag{2a}$$

$$\rho \frac{\mathrm{d}\mathbf{v}}{\mathrm{d}t} + \nabla P + \nabla \left(\frac{B^2}{8\pi}\right) - \frac{(\mathbf{B} \cdot \nabla)\mathbf{B}}{4\pi} = 0 ; \tag{2b}$$

$$\frac{1}{\gamma - 1}\frac{\mathrm{d}P}{\mathrm{d}t} - \frac{\gamma}{\gamma - 1}(P/\rho)\frac{\mathrm{d}\rho}{\mathrm{d}t} + \rho\mathscr{L} - \nabla(K_{\parallel}\nabla_{\parallel}T) = 0\,; \tag{2c}$$

$$P = 2R\rho T\,; \tag{2d}$$

$$\frac{\mathrm{d}\mathbf{B}}{\mathrm{d}t} + \mathbf{B}(\nabla\cdot\mathbf{v}) - (\mathbf{B}\cdot\nabla)\mathbf{v} = 0\,; \tag{3a}$$

and the divergence-free condition for the magnetic field:

$$\nabla\cdot\mathbf{B} = 0\,. \tag{3b}$$

The energy loss per unit mass $\mathscr{L}$ in Equation (2c) is taken to be of the form

$$\mathscr{L}(\rho, T) = (\chi/m_p^2)\rho T^{\varepsilon} - h\,, \tag{4}$$

where the values of the parameters χ and ε are taken from the tables given by Rosner *et al.* (1978), and h is the heating rate per unit mass which is assumed to be constant.

2.2. The Dispersion Relation

We first linearize the basic equations taking a perturbation of the form

$$\Psi = \Psi(x)\exp(nt + ikz)\,, \tag{5}$$

where n is in general complex and k is real and positive. We consider waves propagating only along the magnetic field, i.e., in the z-direction. Two semi-infinite uniform plasma media are chosen which are separated by a non-rigid boundary at $x = 0$, and whose equilibrium states are characterized by ρ_j, T_j, P_j, B_j, and h_j ($j = 1, 2$). The quantities h_j are assumed such that $\mathscr{L}_j = 0$. We confine ourselves to the $x - z$ plane. This will decouple our equations from the Alfvén modes, the polarizations of which are in the y-direction and also from the almost incompressible, Alfvénic surface waves (see discussion in Wentzel, 1979a and also Roberts, 1981a), which occur when $k_y/k_z \gg 1$.

Linearized equations in both the media are then made dimensionless taking the unit of length as k^{-1}, unit of time as $(k^2 P_1/\rho_1)^{-1/2}$ and the unit of magnetic field as B_1. The resulting equations are

$$n\rho + \eta_j\left\{\frac{\mathrm{d}v_x}{\mathrm{d}x} + iv_z\right\} = 0\,; \tag{6a}$$

$$\eta_j n v_x + \frac{\mathrm{d}p}{\mathrm{d}x} + \alpha_j\beta_1\left(\frac{\mathrm{d}b_z}{\mathrm{d}x}\right) - i\alpha_j\beta_1 b_x = 0\,; \tag{6b}$$

$$\eta_j n v_z + ip = 0\,; \tag{6c}$$

$$np + (\sigma_{\rho_j} - \gamma n\delta_j)\rho + \{(n_j/\delta_j)\sigma_{Tj} + \sigma_{K_{\parallel j}}\}T = 0\,; \tag{6d}$$

$$nb_x - i\alpha_j v_x = 0\,; \tag{7a}$$

$$nb_z + \alpha_j \left(\frac{dv_x}{dx}\right) = 0\,, \tag{7b}$$

where $\eta_j = \rho_j/\rho_1$, $\alpha_j = B_j/B_1$, $\delta_j = T_j/T_1$.

The parameter β_1 is defined as two times the inverse of the conventional plasma-beta in medium 1, i.e., $\beta_1 = \gamma(V_{A_1}/C_1)^2$, where V_{A_1} = Alfvén speed in medium 1 and C_1 = acoustic speed in medium 1. The dimensionless terms representing radiative energy loss and energy dissipation due to thermal conductivity are:

$$\sigma_{\rho_j} = \frac{h_j \gamma^{3/2}(\gamma - 1)}{kC_1^3}\,; \qquad \sigma_{Tj} = \varepsilon_j \sigma_{\rho_j}\,;$$

$$\sigma_{K_{\parallel j}} = \frac{(\gamma - 1)kK_{\parallel j}\gamma^{1/2}}{2R\rho_1 C_1} \quad \text{and} \quad \chi_{Rj} = \sigma_{\rho_j}/\sigma_{\rho_1}\,.$$

In the above units we write:

$$\eta_1 = \alpha_1 = \chi_{R_1} = \delta_1 = 1 \quad \text{and} \quad \eta_2 = \eta;\ \chi_{R_2} = \chi_R;\ \delta_2 = \delta\,.$$

After algebraic elimination of other variables, we arrive at a single, second-order differential equation in the total pressure (magnetic + plasma) p_T:

$$\frac{d^2 p_T}{dx^2} = m_j^2 p_T\,, \tag{8}$$

where

$$m_j^2 = \frac{(n^2 + \beta_j)\{n^3 + n^2 A_j + n\gamma\delta_j + B_j\}}{\beta_j n^3 + n\gamma\delta_j(n^2 + \beta_j) + \beta_j n^2 A_j + (n^2 + \beta_j)B_j}\,;$$

$$A_j = (\varepsilon_j/\delta_j)\sigma_{\rho_j} + (\sigma_{K_{\parallel j}}/\eta_j)\,; \tag{9}$$

$$B_j = \sigma_{\rho_j}(\varepsilon_j - 1) + \delta_j(\sigma_{K_{\parallel j}}/\eta_j)\,.$$

Since n is complex, m_j are also in general complex. The x-components of velocities are given by

$$v_x = \frac{-n}{\eta_j(n^2 + \beta_j)}\left(\frac{dp_T}{dx}\right). \tag{10}$$

In the two semi-infinite regions defined by $x > 0$ and $x < 0$, solutions of (8) are:

$$p_T = W_j e^{\mp m_j x}\,,$$

with

$$\mathrm{Re}(m_j) > 0\,. \tag{11}$$

Here W_j are arbitrary constants, and the negative and the positive signs in the exponent correspond to $j = 1$ and 2, respectively.

The boundary conditions at $x = 0$ are:

$$v_{x_1} = v_{x_2} \tag{12a}$$

and

$$P_1 + \frac{B_1^2}{8\pi} = P_2 + \frac{B_2^2}{8\pi}\,. \tag{12b}$$

In the afore-mentioned notation the condition (12b) takes the form:

$$\eta\delta = 1 + (\beta_1/2)(1 - \alpha^2)\,. \tag{13}$$

The perturbed form of Equation (13) is:

$$p_{T_1} = p_{T_2}\,. \tag{14}$$

Using Equations (10), (11), (12a), and (14), we arrive at the following dispersion relation:

$$(n^2 + \beta_1)m_2 = -\eta(n^2 + \beta_2)m_1\,. \tag{15}$$

In the adiabatic limit ($\sigma_{\rho_j} = \sigma_{K_{\parallel j}} = 0$) $n = i\omega$ and Equation (15) agrees with Equation (24) of Roberts (1981a). In the non-adiabatic case m_1 and m_2 are complex and the modes represented by the solutions of Equation (15) are not purely evanescent on the two sides of the interface. We can still call them as 'surface modes' if $\mathrm{Re}(m_j) \gg |\mathrm{Im}(m_j)|$ ($j = 1, 2$), that is, if the amplitude of the waves decay considerably within a distance equal to the reciprocal of the wave vector in the x-direction. In our numerical calculations, we verify this condition for each solution.

3. Discussion of the Dispersion Relation and Its Asymptotic Limits

Squaring of Equation (15), cancellation of the factors $(n^2 + \beta_1)$ and $(n^2 + \beta_2)$ and cross multiplication ultimately leads to an eighth-degree polynomial equation in n:

$$\sum_{i=0}^{8} a_i n^i = 0\,, \tag{16}$$

whose coefficients a_i are given below:

$$a_0 = B_2H_1 - \eta^2 B_1H_2\,,$$

$$a_1 = (\gamma\delta H_1 + B_2G_1) - \eta^2(\gamma H_2 + B_1G_2)\,,$$

$$a_2 = (A_2H_1 + B_2F_1 + \gamma\delta G_1) - \eta^2(A_1H_2 + B_1F_2 + \gamma G_2)\,,$$

$$a_3 = (H_1 + A_2G + \gamma\delta F_1 + B_2E_1) - \eta^2(H_2 + A_1G_2 + \gamma F_2 + B_1E_2)\,,$$

$$a_4 = (G_1 + A_2F_1 + \gamma\delta E_1 + B_2D_1) - \eta^2(G_2 + A_1F_2 + \gamma E_2 + B_1D_2)\,,$$

$$a_5 = (F_1 + A_2E_1 + \gamma\delta D_1 + B_2C_1) - \eta^2(F_2 + A_1E_2 + \gamma D_2 + B_1C_2),$$
$$a_6 = (E_1 + D_1A_2 + \gamma\delta C_1) - \eta^2(E_2 + D_2A_1 + \gamma C_2),$$
$$a_7 = (D_1 + C_1A_2) - \eta^2(D_2 + C_2A_1),$$
$$a_8 = C_1 - \eta^2 C_2,$$

where

$$C_j = \beta_j + \gamma\delta_j; \qquad D_j = B_j + \beta_j A_j^2;$$
$$E_j = \beta_j(C_j + \gamma\delta_j); \qquad F_j = \beta_j(D_j + B_j);$$

and

$$G_j = \gamma\delta_j\beta_j^2; \qquad H_j = \beta_j^2 B_j.$$

Numerical solution of Equation (16) yields, in general, two complex conjugate pairs of 'physical' roots, i.e., those satisfying both the 'original' (unsquared) dispersion relation (15) and the condition of vanishing perturbation at infinity in both directions. The modes given by these roots are classified as the 'slow' and the 'fast' surface modes depending upon their phase speeds.

Before giving numerical results we first discuss the effect of radiative loss terms alone on the surface modes under some asymptotic conditions in terms of parameters α_j and β_j ($j = 1, 2$). Thus we drop the thermal conductivity terms in Equation (9). We refer to the cooler of the two regions as medium 1 (i.e., T_2/T_1 or $\delta > 1$) and consider the following cases:

Case A: $B_1^2/8\pi \ll P_1$ and $B_2^2/8\pi \ll P_2$

From Equation (12b), $P_1 \sim P_2 \gg B_1^2/8\pi$, $B_2^2/8\pi$.

For convenience of the discussion, we take $B_1 \approx B_2$ and $P_1 \approx P_2$. Hence, in our present notation: $\beta_1 \to 0$, $\alpha^2 \approx 1$, $\eta \approx 1/\delta$, and $\beta_2 \approx \delta\beta_1 \to 0$. In this case, dispersion relation for adiabatic conditions (Wentzel, 1979a; Roberts, 1981a) gives only a slow surface mode with frequency

$$n^2 \approx -\frac{\beta_2 + \beta_2/\eta}{1 + 1/\eta} \approx -\frac{2\beta_2}{1 + \delta}. \tag{17}$$

We expect maximum radiative influence on this mode when the period is of the same order of the radiative cooling time, i.e., $\sigma_{\rho_1} \sim \sigma_{\rho_2} \sim |n| \sim \beta_1^{1/2}$. Now for $\beta_1 \to 0$, the limiting forms of m_1^2 and m_2^2 are:

$$m_j^2 = \frac{(n^2 + \beta_j)\{n\gamma\delta_j + \rho_{\rho_j}(\varepsilon_j - 1)\} + \vartheta(\beta_j^{5/2})}{(n^2 + \beta_j)\{n\gamma\delta_j + \sigma_{\rho_j}(\varepsilon_j - 1)\} + \vartheta(\beta_j^{5/2})} = 1 + \vartheta(\beta_j). \tag{18}$$

Equation (18) gives the same dispersion relation as that in the adiabatic case. The reason for this can be understood if we compare each of the fractional perturbations in the gas variables ($\delta P/P$, etc.) in the two media to the corresponding perpendicular velocity, which must be non-zero in the surface modes. From Equations (6a) to (7b) we obtain

$$mn(\delta P/P) = \pm \{n^2 + \beta(1 - m^2)\} v_x , \tag{19a}$$

$$mn^3(\delta\rho/\rho) = \mp \{(1 - m^2)(n^2 + \beta)\} v_x , \tag{19b}$$

and

$$mn(\delta T/T) = \pm [\{n^2 + \beta(1 - m^2)\} + \frac{1}{n^2}(1 - m^2)(\beta + n^2)] v_x . \tag{19c}$$

For m^2 given by (18), $|\delta P/P| \sim |\delta\rho/\rho| \sim |\delta T/T| \ll |v_x|$.

Since the radiative processes affect the stability of the modes only through the first-order perturbations of the thermodynamic variables, we get only neutrally stable surface modes in case A. This can also be seen in the results obtained by numerical solution of Equation (16) which are shown in Figure 1. The growth rate of the overstable slow surface mode decreases monotonically with the decrease of β_1 (and, hence, of β_2) for fixed values of α^2 and δ and vanishes for very low values of β_1.

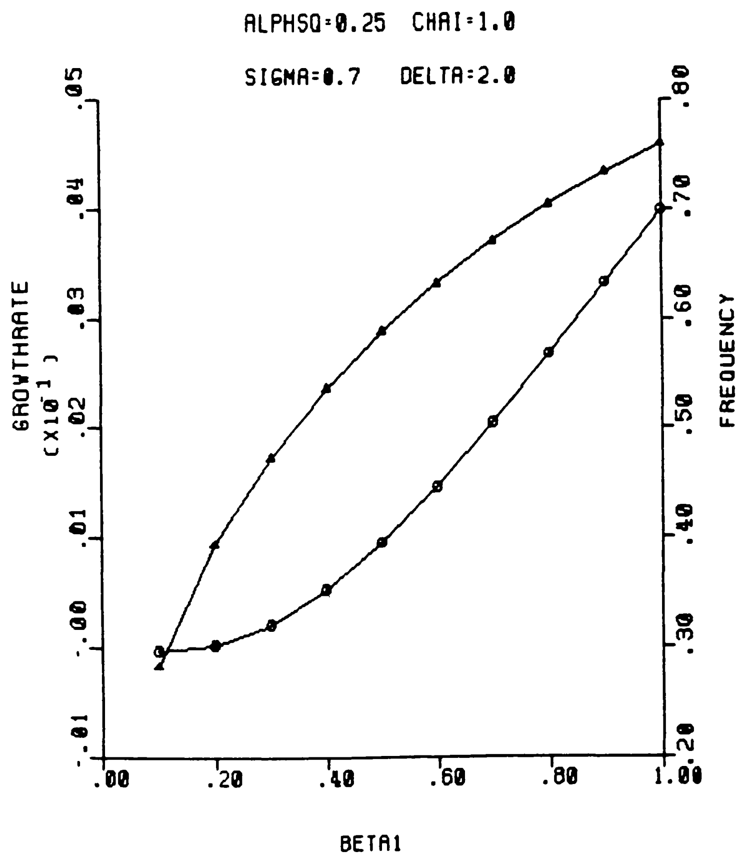

Fig. 1. Growth rate (represented by ○) and frequency (represented by △) of the slow surface mode as functions of β_1 (BETA 1) for fixed values of α^2 (ALPHSQ), δ (DELTA), χ_R (CHAI), and σ_{ρ_1} (SIGMA). Note that the growth rate tends to zero in the asymptotic limit of $\beta_1 \to 0$.

Case B: $B_1^2/8\pi \gg P_1$ and $B_2^2/8\pi \gg P_2$

For simplicity we take $B_1^2 \approx B_2^2$ and $P_1 \approx P_2$.

Hence, in our notation: $\beta_1 \to \infty$, $\alpha^2 \approx 1$, $\eta \approx 1/\delta$, and $\beta_2 \approx \delta\beta_1$. In the adiabatic situation Wentzel and Roberts have shown that pure surface modes are not possible in this limit. However, they discuss a one-sided surface wave with $n = \pm i\sqrt{\beta_1}$ in medium 2 terminated by an Alfvén wave with $m_1^2 = 0$ in medium 1. For periods comparable to radiative loss time, i.e., for $|n| \sim \beta_1^{1/2} \sim \sigma_{\rho_1} \sim \sigma_{\rho_2}$,

$$m_j^2 = \frac{(n^2 + \beta_j)\,[\{n + \varepsilon_j\sigma_{\rho_j}/\delta_j\} + \vartheta(\beta_j^{-1/2})]}{\beta_j\{n + \varepsilon_j\sigma_{\rho_j}/\delta_j\} + \vartheta(\beta_j^{1/2})}$$

$$= (n^2 + \beta_j)\left[\frac{1}{\beta} + \vartheta(\beta_j^{-2})\right]. \tag{20}$$

With the help of Equation (20), Equation (15) can be written as

$$m_1 m_2\left[\frac{m_1}{1/\beta_1\{1 + \vartheta(\beta_1^{-1})\}} + \frac{\eta m_2}{1/\beta_2\{1 + \vartheta(\beta_2^{-1})\}}\right] = 0\,, \tag{21}$$

which cannot be satisfied together with condition (11). Hence, the only permissible solution is $m_1 = 0$ and $n^2 = -\beta_1$ which makes the one-sided surface mode completely decoupled from radiative effects. For m_j^2 given by Equation (20), Equation (19) gives $|\delta P/P| \sim |\delta\rho/\rho| \sim |\delta T/T| \ll v_x|$ in both medium 1 and 2 for this one-sided surface mode, which explains the above results.

Case C: $B_1^2/4\pi P_1 \gg 1$, $B_2^2/4\pi P_2 \ll 1$, $B_2^2/B_1^2 \ll 1$, and $B_1^2/8\pi \approx P_2$.

For simplicity, we assume $\alpha^2 \sim 1/\beta$ and $\delta \sim$ finite.

Then, $\beta_1 \approx 2\eta\delta \to \infty$; $\eta \sim \beta_1$ and $\beta_2 = (\alpha^2/\eta)\beta_1 \sim \beta_1^{-1} \to 0$.

In the adiabatic situation (Roberts, 1981a), we have a slow surface mode with $n^2 \approx -\gamma$ and a fast surface mode with $n^2 \approx -[(\sqrt{1 + \gamma^2} - 1)2\delta]/\gamma$.

In the non-adiabatic situation and for $|n| \sim \sigma_{\rho_1} \sim \sigma_{\rho_2} =$ finite, approximate expressions for m_1^2 and m_2^2 are given by:

$$m_1^2 \approx \frac{(n^2 + \beta_1)\,\{n^3 + n^2\varepsilon_1\sigma_{\rho_1} + \gamma n + \sigma_{\rho_1}(\varepsilon_1 - 1)\}}{\beta_1\{n^3 + \varepsilon_1\sigma_{\rho_1}n^2 + \gamma n + \sigma_{\rho_1}(\varepsilon_1 - 1)\}}$$

and

$$m_2^2 \approx \frac{n^3 + n^2(\varepsilon_2\sigma_{\rho_2}/\delta) + \gamma\delta n + \sigma_{\rho_2}(\varepsilon_2 - 1)}{n\gamma\delta + \sigma_{\rho_2}(\varepsilon_2 - 1)}\,. \tag{22}$$

After rearrangement of the terms, the 'squared' dispersion relation takes the form:

$$\{n^3 + n^2\varepsilon_1\sigma_{\rho_1} + \gamma n + \sigma_{\rho_1}(\varepsilon_1 - 1)\}\,\{n^5(\gamma\delta) + n^4\sigma_{\rho_2}(\varepsilon_2 - 1) - (4\delta^2)n^3 - (4\delta)(\varepsilon_2\sigma_{\rho_2})n^2 - (4\gamma\delta^3)n - (4\delta^2)\sigma_{\rho_2}(\varepsilon_2 - 1)\} \approx 0\,. \tag{23}$$

The roots given by the first parenthesis represent the slow surface mode with an 'unphysical' root. For the slow surface mode, power expansions (Field, 1965) in regions $\sigma_{\rho_1} \ll 1$ and $\sigma_{\rho_1} \gg 1$ give (up to the first-order terms):

$$n \approx \frac{\sigma_{\rho_1}\{(\varepsilon_1 - 1) - \gamma\varepsilon_1\}}{2\gamma} \pm i\sqrt{\gamma}, \tag{24a}$$

and

$$n \approx \pm\sqrt{\frac{1-\varepsilon_1}{\varepsilon_1} + \frac{1}{\varepsilon_1^2\sigma_{\rho_1}}\left\{\frac{(\varepsilon_1 - 1) - \gamma\varepsilon_1}{2\gamma}\right\}}, \tag{24b}$$

respectively. Thus, we see that the criterion of overstability for the slow surface mode agrees with Fields' criterion of medium 1, i.e.,

$$\varepsilon_1 < -\frac{1}{\gamma - 1}. \tag{25}$$

This result can be explained with the help of Equations (14) and (22). For the slow surface mode m_1^2 and m_2^2 are both finite and $m_1^2 \not\approx (n^2 + \beta_1)/\beta_1$. In medium 1 this gives $|\delta P/P| \sim |\delta\rho/\rho| \sim |\delta T/T| \gg v_x|$, while in medium 2, $|\delta P/P| \sim |\delta\rho/\rho| \sim |\delta T/T| \sim |v_x|$. Since the perturbations in the gas variables are much larger in medium 1 than in medium 2, the thermal stability of this particular mode is determined mainly by the radiative properties of medium 1.

The second parenthesis of Equation (23) yields one 'unphysical' root, two 'spurious' roots and the fast surface mode. As above, a power series expansion for the fast surface mode in the region $\sigma_{\rho_1} \ll 1$ gives

$$n \approx -(0.1029)(1/\delta)\sigma_{\rho_2}(\varepsilon_2 + 1.5) \pm i(1.10641)\delta^{1/2}, \tag{26a}$$

where we have chosen $\gamma = \frac{5}{3}$ to avoid cumbersome expressions involving γ.

We see that in this case the overstability criterion for the fast surface mode is $\varepsilon_2 < -1.5$ which is same as Field's criterion in medium 2. For the series expansion in the region $\sigma_{\rho_2} \gg 1$, we take $\gamma = \frac{5}{3}$ and also $\varepsilon_2 = -2.00$, for simplicity of illustration, and obtain:

$$n \approx (0.0165)(\sigma_{\rho_2} - 1)\delta^2 \pm i(1.0346)\delta^{1/2}. \tag{26b}$$

From Equations (26a) and (26b) we see that the growth rates and the overstability criterion for the fast surface mode is predominantly determined by the radiative losses in medium 2. This is so because Equations (22) give $m_1^2 \approx (n^2 + \beta_1)/\beta_1 = 1 + \vartheta(\beta_1^{-1})$ and $m_2^2 =$ finite, leading to $|\delta P/P| \sim |\delta\rho/\rho| \sim |\delta T/T| \ll |v_x|$ in medium 1 and $|\delta P/P| \sim |\delta\rho/\rho| \sim |\delta T/T| \sim |v_x|$ in medium 2.

In Figures 2, 3, and 4 we illustrate the dependence of growth rates and frequencies of the two surface modes on the parameters σ_{ρ_1}, δ, and β_1 under various conditions. The figures are drawn from the solution of Equation (16) for arbitrarily chosen parameters

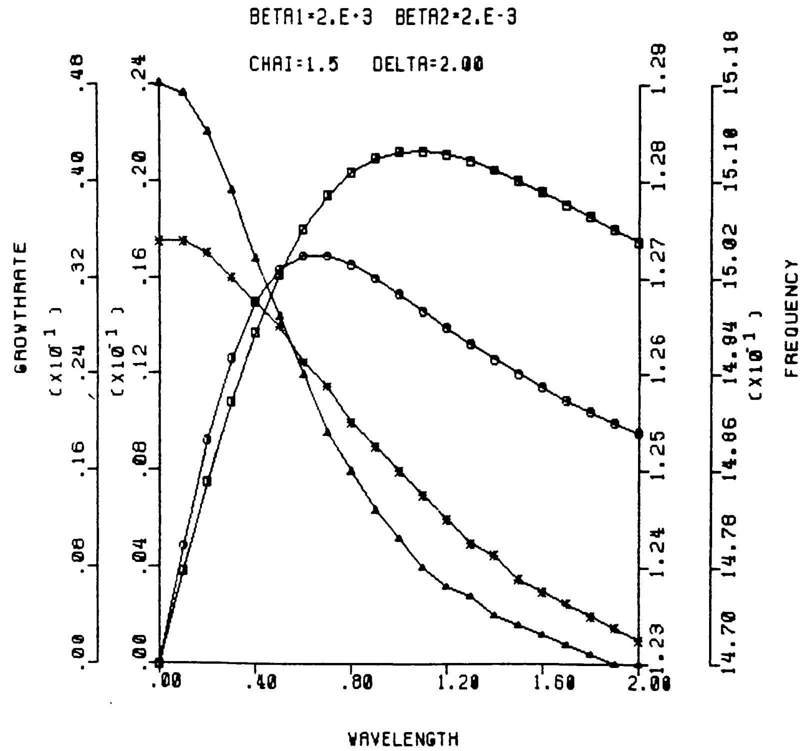

Fig. 2. Growth rate and frequencies of the slow and the fast modes as functions of the dimensionless wavelength σ_{ρ_1} in the limit of β_1(BETA 1) $\to \infty$ and β_2(BETA 2) $\to 0$ represented by $\beta_1 = 2 \times 10^3$ and $\beta_2 = 2 \times 10^{-3}$, respectively. Values chosen for χ_R(CHAI) and δ(DELTA), are indicated. The dimensionless growth rates for the slow and the fast modes are represented by ○ and □, respectively, and refer to the vertical scales on the left side. Corresponding frequencies are shown by △ and ∗ referring to the vertical scales on the right side. On either side, the first scale is for the slow mode and the second one is for the fast mode. Note that the ranges of values on the frequency axes are quite small showing that the frequencies are insensitive to the changes of $\sigma_{\rho 1}$.

$\varepsilon_1 = -2.00$ and $\varepsilon_2 = -1.00$ and $\chi_R = 1.50$. In Figure 2 growth rate of the slow(/fast) surface mode increases linearly with $\sigma_{\rho_1}(/\sigma_{\rho_2})$ in the quasi-adiabatic domain of small wavelengths (σ_{ρ_1} and $\sigma_{\rho_2} \ll 1$) where the radiative cooling times of the two media are much longer than the sound travel times which, in turn, have the same orders of magnitude as the periods of the two waves. On the other hand, in the long wavelength region ($\sigma_{\rho_1}, \sigma_{\rho_2} \gg 1$), the radiative time-scales are shorter than the periods, and this results in a damping of the surface modes. Frequencies of the modes are mainly determined by the nonradiative properties of the media and, therefore, vary rather slowly with σ_{ρ_1}.

In a similar manner one can explain the variation of the growth rates of the surface modes with the temperature ratio δ of the two media. An increase in δ and the corresponding decrease in the sound travel time in medium 2, for a fixed wavelength of perturbation, decreases the growth of the fast surface mode in the small wavelength limit. On the other hand, in the large wavelength limit, the sound travel time tends to be comparable to the radiative cooling time of medium 2, and the growth rate increases. This is shown in Figures 3(a) and 3(b). Here the growth rate of the slow surface mode seems to be insensitive to the parameter δ. This is understandable since δ is merely T_2

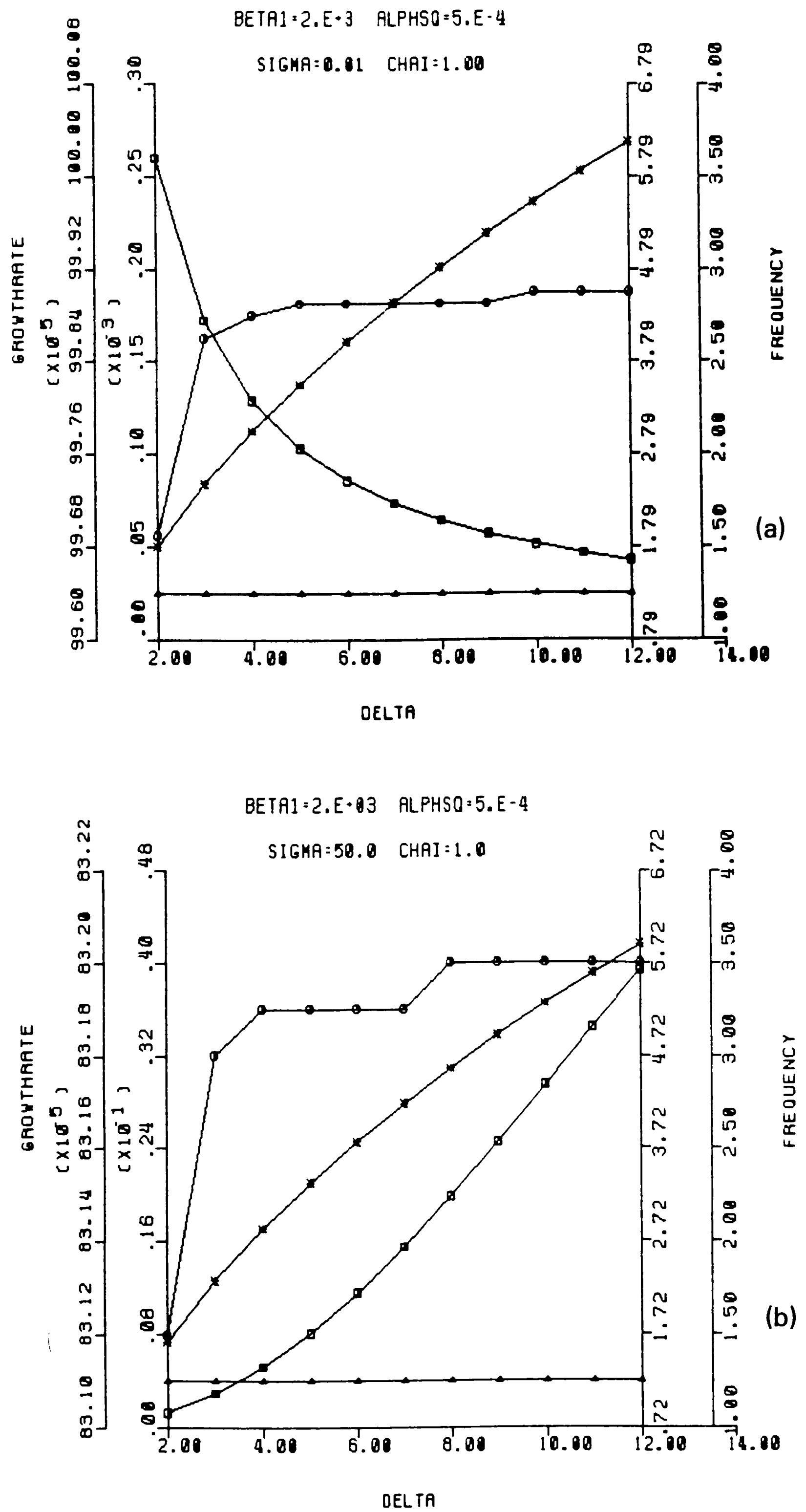

Fig. 3a–b. Growth rates and frequencies of the slow and the fast modes as functions of the temperature ratio δ (DELTA) of the two media in the asymptotic limit $\beta_1 \rightarrow \infty$ ($= 2 \times 10^3$) and $\beta_2 \rightarrow 0$ as implied by α^2(ALPHSQ)$\rightarrow 0$ ($\simeq 5 \times 10^{-4}$). The small wavelength limit (a) is represented by the value σ_{ρ_1}(SIGMA) $= 10^{-2}$, while the large wavelength limit (b) is represented by the value $\sigma_{\rho_1} = 50.0$. The vertical axes and the symbols are similar to those in Figure 2. Apparent sudden jumps in the growth rates of the slow surface mode are artifacts of the plotting programme.

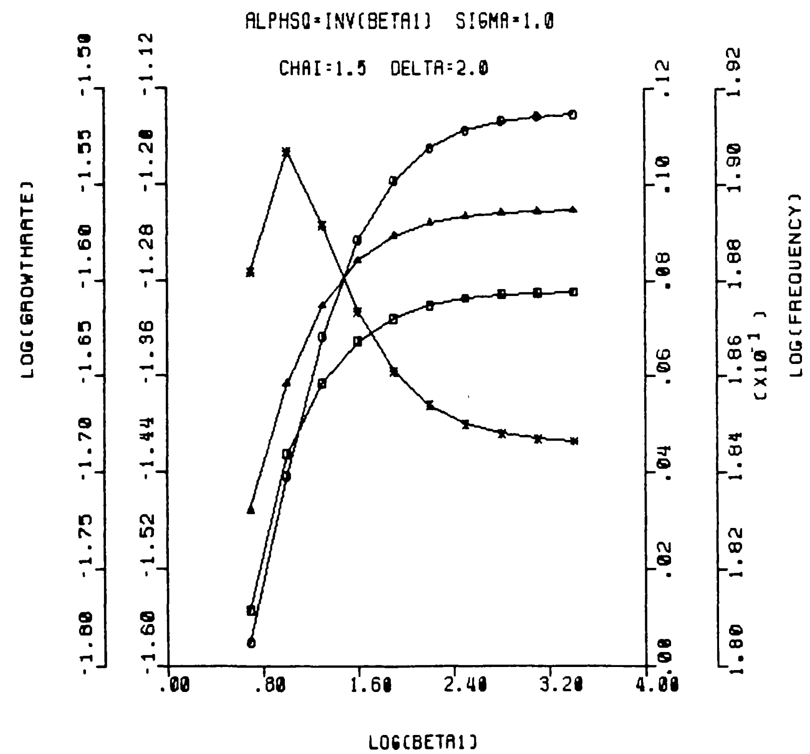

Fig. 4. Growth rates and frequencies of the slow and the fast surface modes as functions of β_1 in logarithmic scales, where an increase of β_1 is accompanied by a decrease of α^2(ALPHSQ) and, therefore, of β_2. Fixed values are chosen for σ_{ρ_1}, χ_R(CHAI), and δ(DELTA). The vertical axes and the symbols are similar to those in Figure 2.

normalized in units of T_1, but the slow surface mode overstability is independent of T_2.

Figure 4 shows the variations of the growth rates and the frequencies of the two surface modes as β_1 and β_2 approach asymptotic values ∞ and 0, respectively, from intermediate values. The growth rates of both modes increase with increasing β_1 and ultimately become independent of β_1, as predicted by Equation (23). Physically this shows that the modes become almost completely acoustic in this limit of large β_1.

4. Numerical Results for Two Types of Interfaces

Since pure surface modes are almost stable in case A and non-existent in case B, we present here numerical solution of Equation (16) for the two varieties of discontinuities which fall under the category of case C, i.e., the discontinuities across which the value of β changes appreciably. While doing so we assign for various parameter values which are typical in solar atmosphere. We shall consider the effects of thermal conductivity also. Extrapolating the conclusions of case C in the previous section, we expect that in the presence of thermal conductivity the surface modes will be stabilized for wavelengths

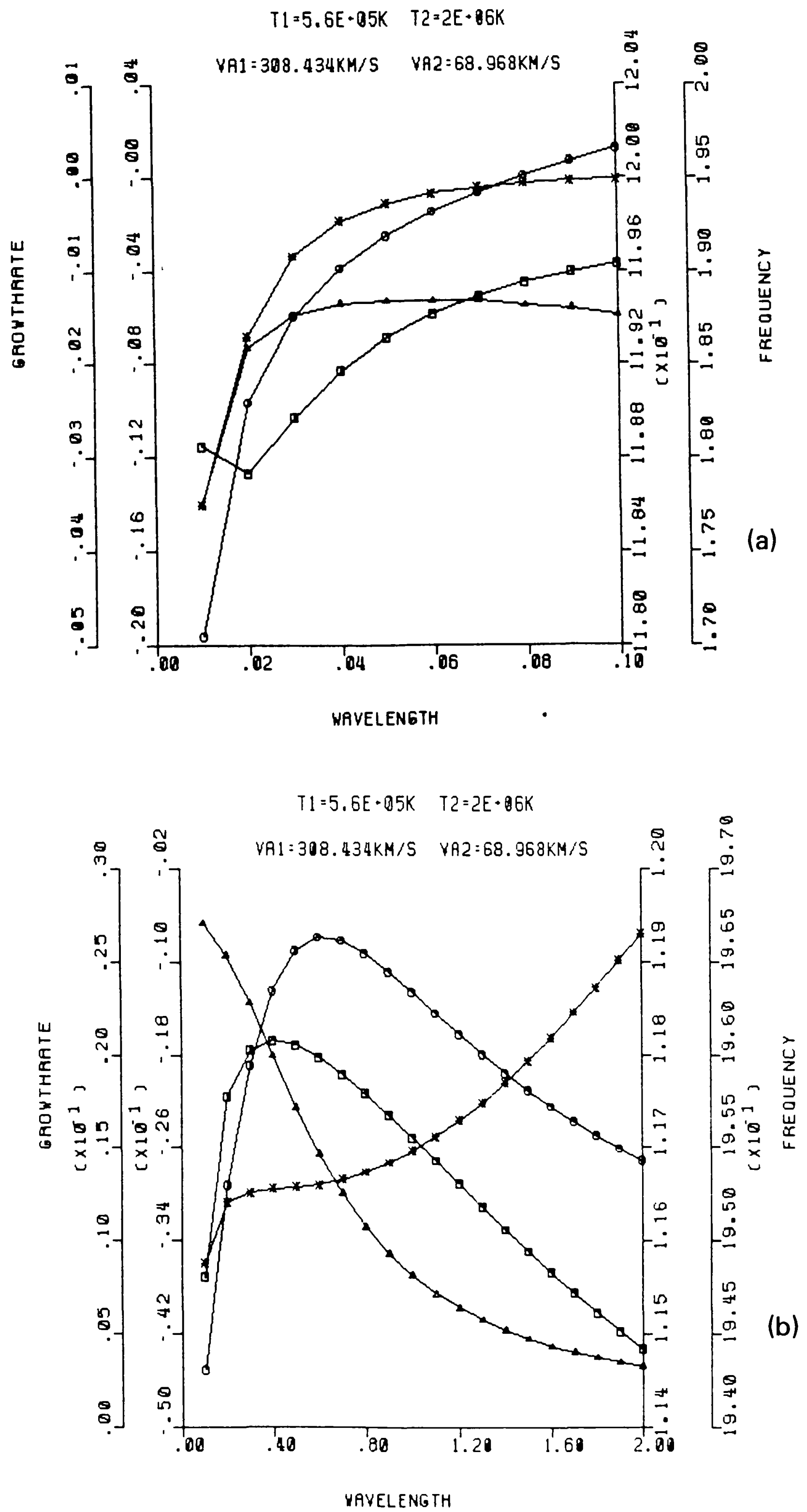

Fig. 5a–b. Effect of radiative loss and thermal conductivity parallel to the magnetic field on the growth rates and frequencies of the surface modes for a situation considered in Section 4.1 and for two ranges of dimensionless wavelengths. (a) shows the cut-off in the short wavelength limit for the overstability of the slow surface mode. The values chosen for T_1, T_2, V_{A_1}(VA1) and V_{A_2}(VA2) are as given. The axes and symbols are similar to those in Figure 2.

below the critical wavelengths given by Field (1965), viz.,

$$\sigma_{\rho_j} < -\left\{\sigma_{K_{\|j}} \Big/ \left(\varepsilon_j + \frac{1}{\gamma - 1}\right)\right\}, \tag{27}$$

with $j = 1$ and 2, respectively.

The situations considered are the following.

4.1. The field in the cooler medium is stronger

Numerical results in this case are illustrated in Figures 5(a) and 5(b). The temperatures and the Alfvén velocities are given in the figures. The temperatures correspond to $\varepsilon_1 = -2.0$ and $\varepsilon_2 = -\frac{2}{3}$ (Rosner *et al.*, 1978). Consequently the fast surface mode is stable for any value of σ_{ρ_2} and $\sigma_{K_{\|2}}$ (ref. Equation (27)). The onset of overstability for the slow surface mode occurs at a wavelength corresponding to $\sigma_{\rho_1} = 0.08$, while the critical wavelength given by Equation (27) is $\sigma_{\rho_{1c}} = 0.078$. The fastest growing mode has a frequency of 0.85 mHz, and a wavelength of 1.3×10^5 km, while the growth time is 2.3 hr. The *e*-folding distances for this mode are 4000 km in the cooler medium and 25 500 km in the hotter medium.

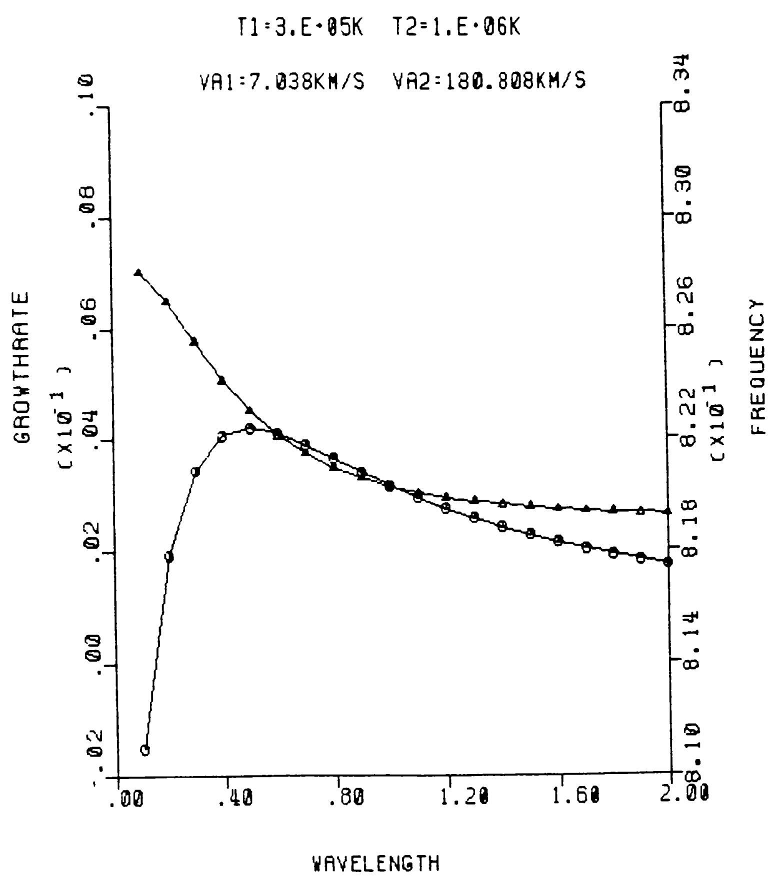

Fig. 6. Effect of radiative loss and parallel thermal conductivity on the growth rates and frequencies of the surface modes in the situation considered in Section 4.2. The axes and symbols are similar to those in Figure 5.

4.2. The field in the hotter medium is stronger

Figure 6 illustrates the numerical results for such a case. Only the slow surface mode can exist in this case and the onset of overstability of this mode occurs at $\sigma_{\rho_1} = 0.13$. This also happens to be close to the critical wavelength $\sigma_{\rho_{1c}} = 0.124$ given by Equation (27). In this case the fastest growing mode has a wavelength of 650 km, a frequency of 89.5 mHz, and growth time of 5.8 min. The penetration distances in the two media are 140 km in medium 1 and 102 km in medium 2.

5. Summary and Discussion

In the above section we have examined the thermal stability of a sharp discontinuity in a magnetic plasma. The conclusion of the study is that under suitable conditions an 'in situ' generation of surface waves along such a discontinuity is possible through the overstability caused by radiative heat-losses. In Section 3 we have shown that this overstability is appreciable when the plasma-beta on the two sides of the interface are substantially different. The overstability further requires that the medium in which the surface mode is more compressible should satisfy the Field's criterion. In solar coronal plasma this implies that the temperature of the corresponding region should lie in a narrow range of $\sim 10^{5.4}$–$10^{5.75}$ K. This condition might be satisfied near the surfaces of the coronal magnetic structures like a 'cool-core coronal loop' or the 'prominence-corona interface'. The example given in Section 4.1 might simulate the situation at the interface between a 'cool-core–hot-sheat coronal loop' and the ambient medium. The excitation and growth of the surface waves could possibly lead to turbulence at such an interface. In the case of prominence-corona interface, the low resolution of magnetic observations and uncertainties in theoretical models do not enable us to decide whether the conditions in Section 4.1 or 4.2 are mor realistic. However, the general increase of turbulent velocity towards the edge of the prominence (Hirayama, 1985) might be construed as an indication of the surface overstability in this case also.

The excitation of surface waves through overstability might also facilitate transfer of energy and momentum from the lower corona to higher corona and interplanetary space.

Finally, it must be remembered that the aforementioned results and conclusions apply only to waves of wavelength much smaller than the thickness of the coronal magnetic structures, in which case the structures can be approximated as a single interface (Roberts, 1981b; Edwin and Roberts, 1982). For more general applicability one must consider the effect of finite thickness of the structures and study both surface as well as bulk modes in relation to the thermal stability.

Acknowledgements

We are grateful to Dr K. N. Nagendra and an unknown referee for their comments on an earlier version of this paper. We thank Dr S. Giridhar, Mr V. C. Mouli, Mr K. E. Rangarajan, and Mr D. M. Rao for helping us in improving computation and plotting programme.

References

An, C. H.: 1984, *Astrophys. J.* **276**, 352.
Bodo, G., Ferrari, A., Massaglia, S., and Rosner, R.: 1986, preprint.
Edwin, P. M. and Roberts, B.: 1982, *Solar Phys.* **76**, 239.
Field, G.: 1965, *Astrophys. J.* **142**, 531.
Gordon, B. E. and Hollweg, J. V.: 1983, *Astrophys. J.* **266**, 373.
Heyvaerts, J.: 1974, *Astron. Astrophys.* **37**, 65.
Hildner, E.: 1974, *Solar Phys.* **35**, 123.
Hirayama, T.: 1985, *Solar Phys.* **100**, 415.
Ionson, J. A.: 1978, *Astrophys. J.* **226**, 650.
Ionson, J. A.: 1985, *Solar Phys.* **100**, 289.
Priest, E. R.: 1978, *Solar Phys.* **35**, 123.
Priest, E. R.: 1982, *Solar MHD*, D. Reidel Publ. Co., Dordrecht, Holland.
Rae, I. C. and Roberts, B.: 1981, *Geophys. Astrophys. Fluid Dynamics* **18**, 197.
Roberts, B.: 1981a, *Solar Phys.* **69**, 27.
Roberts, B.: 1981b, *Solar Phys.* **69**, 39.
Rosner, R., Tucker, W. H., and Viana, G. S.: 1978, *Astrophys. J.* **220**, 643.
Somasundaram, K.: 1983, Ph.D. Thesis, Indian Institute of Science, Bangalore, India.
Somasundaram, K. and Uberoi, C.: 1982, *Solar Phys.* **81**, 19.
Spitzer, L., Jr.: 1962, *Physics of Fully Ionized Gases*, 2nd ed., Interscience Publishers, New York.
Wentzel, D. G.: 1979a, *Astrophys. J.* **227**, 319.
Wentzel, D. G.: 1979b, *Astron. Astrophys.* **76**, 20.
Wentzel, D. G.: 1979c, *Astrophys. J.* **223**, 756.